2013 European Control Conference (ECC)
July 17-19, 2013, Zürich, Switzerland.

Optimal Energy Management for a Mechanical-Hybrid Vehicle with Cold Start Conditions

Koos van Berkel, Wouter Klemm, Theo Hofman, Bas Vroemen, Maarten Steinbuch

Abstract— **This paper presents the design of an optimal Energy Management Strategy (EMS) for a hybrid vehicle that starts with a cold powertrain. The cold start negatively affects the combustion and transmission efficiency of the powertrain, caused by the higher frictional losses due to increased hydrodynamic viscosity effects. The excess fuel consumption of the engine and the excess power loss of the transmission are modeled by static relations as a function of the lubrication oil temperature. The thermodynamics in the powertrain during the heating period of the powertrain is approximated by a first-order dynamic model. The main design criterion for the optimal EMS is the minimization of the overall fuel consumption over a pre-defined driving cycle. Dynamic programming is used to find the globally optimal solution for six representative driving cycles. The results show that the cold start has a significant impact on the fuel consumption of the hybrid vehicle, yet its influence on the optimal EMS is negligible.**

Index Terms— **Automotive, Optimal control, Modeling**

I. Introduction

Hybrid powertrains use a secondary power source to improve the fuel consumption of the primary power source, which is usually an internal combustion engine. The secondary power source is able to store energy from the engine and to exchange energy with the propelled vehicle. The power flows between the engine, the secondary power source, and the vehicle are controlled at powertrain level by an Energy Management Strategy (EMS), which aims at minimizing the overall fuel consumption. For the overall EMS design, it is useful to know the globally optimal solution for a pre-defined driving cycle, as it provides a benchmark for the fuel saving potential of the hybrid powertrain and gives insights in the optimal utilization of the secondary power source [1]. Most EMS designs described in the literature assume that the hybrid powertrain is already at its operating temperature at the start of a driving cycle, when the combustion and transmission efficiencies are already relatively high. The warm start conditions may be realistic after driving a few kilometers, but obviously not when the car has been parked for a few hours.

This work is a part of the mecHybrid project which is a common project of DTI, Punch Powertrain, CCM, Bosch, SKF, and TU/e. The project is partly funded by the Dutch Ministry of Economic Affairs, Provincie Noord-Brabant and SRE.

K. van Berkel, T. Hofman, and M. Steinbuch are with the Department of Mechanical Engineering, Eindhoven University of Technology, P.O. box 513, 5600 MB Eindhoven, The Netherlands, Phone: +31 40 247 2811, Fax: +31 40 246 1418, k.v.berkel@tue.nl, t.hofman@tue.nl, m.steinbuch@tue.nl.

W. Klemm is with FEV, Neuenhofstasse 181, 52078 Aachen, Germany.klemm@fev.com.

B. Vroemen is with Drivetrain Innovations, Croy 46, 5653 LD Eindhoven, The Netherlands, vroemen@dtinnovations.nl.

A. Cold start conditions

A low powertrain temperature has a negative impact on the fuel consumption and the transmission efficiency caused by higher frictional losses in the engine and CVT due to increased hydrodynamic viscosity effects [2]–[4] and the need of a richer air/fuel mixture to overcome poor combustion [5]. The impact is especially high in the first few minutes of the thermodynamic transient and gradually decreases with increasing temperature [6], [7]. For hybrid vehicles, this effect holds for a longer time, due to intermittent and relatively very efficient engine operation [8], [9]. Various solutions exist to shorten the heating time, *e.g.*, by using an external heater [6], by using exhaust gas heat [10]–[12], or by slower heating of the passenger compartment [13]. Hybrid vehicles can use their energy buffer to shorten the heating time of the powertrain [14], [15], by extending the design space of the EMS with an additional temperature state.

B. Approach and outline

This paper designs an optimal EMS for a hybrid powertrain to investigate the influence of the cold start conditions on i) the fuel consumption, ii) the fuel saving potential of the hybrid powertrain, and iii) the associated optimal EMS. The approach is as follows: the powertrain temperature is modeled by a first-order model for the relevant heating range. The excess fuel consumption of the engine and the excess power dissipation of the transmission are modeled by temperature-dependent multiplier functions, which extend the nominal models that are only valid at the operating temperature. These thermodynamic models, of which the key modeling coefficients are identified with test rig experiments, are added to an existing mechanical hybrid powertrain model. The optimal control problem is to minimize the overall fuel consumption for a given driving cycle, subject to the system's kinematics, dynamics, and constraints. The problem is numerically solved using deterministic dynamic programming [16], for both cold and warm start conditions and a set of six representative driving cycles.

The outline is given as follows: Section II describes the modeling of the thermodynamics, whereas Section III describes the modeling of the motion dynamics. Section IV formalizes the optimization problem. Section V describes the simulation settings of which the results are discussed in Section VI.

II. THERMODYNAMIC MODELING

A first-order thermodynamic model of the powertrain temperature is presented for a CVT-based powertrain that is sufficiently accurate for the main thermodynamic effects during the heating period. The temperature-dependent fuel consumption of the engine and the temperature-dependent power dissipation of the CVT are modeled by static functions. The key modeling coefficients are identified with test rig experiments.

A. Powertrain temperature

The engine converts a significant part of the fuel power P_f (*i.e.*, chemical energy flux) into the effective mechanical power P_e, whereas another part leaves the engine in the form of exhaust gases P_x and convection with the ambient air P_a. The transmission and clutch transmit the mechanical power (P_e) with a favorable rotational speed to the drive shaft (P_d), yet at the expense of frictional and pumping losses in the transmission P_t and slip losses in the clutch P_c. The remainder of the power, *i.e.*, $P_\mathrm{f} - P_\mathrm{x} - P_\mathrm{a} - P_\mathrm{d}$, is converted into heat, which is absorbed and distributed by various heat carrying media in the powertrain. The heater in the passenger compartment is not explicitly considered in this model, as it is controlled by the passenger and therefore not relevant for the EMS design. The considered power flows are schematically depicted in Fig. 1.

The majority of the overall heat production in the powertrain is due to combustion and friction of moving parts in the engine. The combustion heat in the combustion chambers is mainly absorbed by the coolant, which subsequently, exchanges this heat with other media such as the lubrication oils of the engine and transmission, and the metal parts of the powertrain. During the powertrain heating period, the coolant temperature is higher than that of the lubrication oils (see, Fig. 4), so that heat is distributed from the coolant to the lubrication oils (*i.e.*, the coolant is heating). When the coolant is sufficiently heated (around 80° C), the thermostat opens and starts with active control of the coolant temperature, after which the heat is distributed from the lubrication oils to the coolant (*i.e.*, the coolant is cooling). Eventually, the engine oil temperature reaches an equilibrium around 90° C-110° C due to the relatively high friction losses, whereas the transmission oil temperature reaches an equilibrium close to the coolant temperature around 80° C-90° C, due to the relatively low losses under normal driving conditions.

Each thermodynamic process within and between heat carrying media acts at a different time scale, for which detailed thermodynamic models are described in [17]–[19]. For the design of the EMS, however, it is sufficient to describe the heating of the engine oil ϑ_e and the transmission oil ϑ_t at the time scale of several minutes. The relevant temperature range is limited to the range between the ambient temperature $\underline{\vartheta}_\mathrm{p}$ and the (minimum) operating temperature $\overline{\vartheta}_\mathrm{p}$ for which the temperature has negligible influence on the fuel consumption

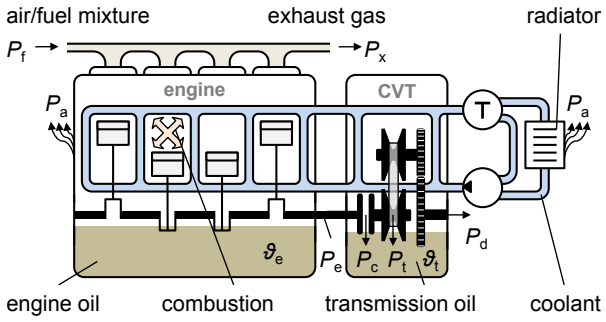

Fig. 1. Schematic overview of the main thermodynamic effects within a CVT-based powertrain.

and transmission losses. As a first order approximation, it is assumed that for the relevant temperature range, i) the thermostat is closed, so the radiator can be neglected, and ii) the engine oil and transmission oil temperatures have approximately the same temperature, since both oils are heated by the same coolant, so it is sufficient to model one overall powertrain temperature ϑ_p, *i.e.*,

$$\vartheta_\mathrm{p} \approx \vartheta_\mathrm{e} \approx \vartheta_\mathrm{t} \qquad \vartheta_\mathrm{p} \in [\underline{\vartheta}_\mathrm{p},\ \overline{\vartheta}_\mathrm{p}] \tag{1}$$

Neglecting the radiator, the thermodynamics can be described with one lumped heat capacity for the powertrain as in [20], by

$$\dot{\vartheta}_\mathrm{p}(t) = \begin{cases} \frac{P_\mathrm{f}(t) - P_\mathrm{x}(t) - P_\mathrm{d}(t) - P_\mathrm{a}(t)}{C_\mathrm{p}} & \text{if } \vartheta_\mathrm{p}(t) < \overline{\vartheta}_\mathrm{p}, \\ 0 & \text{if } \vartheta_\mathrm{p}(t) = \overline{\vartheta}_\mathrm{p} \end{cases}. \tag{2}$$

The effective heat capacity of the powertrain $C_\mathrm{p} = m_\mathrm{p} c_\mathrm{p} c_\mathrm{h}$, is a function of the powertrain mass m_p, its specific heat coefficient c_p, and a heating coefficient $0 < c_\mathrm{h} \leq 1$. The heating coefficient corrects for the faster heating of the lubrication oils than that of other media in the powertrain such as the metal housing, and is experimentally identified in the sequel. The fuel power P_f depends on the operating point (*i.e.*, speed and torque) of the engine and the powertrain temperature, as will be described in the sequel. The exhaust gas heat is approximated by a fraction of the fuel power, which linearly decreases with the engine speed ω_e, *i.e.*, $P_\mathrm{x} = (c_{\mathrm{x},1} - c_{\mathrm{x},2}\omega_\mathrm{e})P_\mathrm{f}$, where $c_{\mathrm{x},1}$ and $c_{\mathrm{x},2}$ are constant coefficients as described in [21]. The drive shaft power equals the mechanical power produced by the engine minus the transmission and clutch losses, *i.e.*, $P_\mathrm{d} = P_\mathrm{e} - P_\mathrm{t} - P_\mathrm{c}$. The convective heat transfer to the ambient air is modeled by $P_\mathrm{a} = c_\mathrm{a} A_\mathrm{a} (\vartheta_\mathrm{p} - \underline{\vartheta}_\mathrm{p})$, where c_a is the heat transfer coefficient to the ambient air and A_a the active heat-exchange area. The set of realistic parameters is listed in Table I.

B. Temperature-dependent fuel consumption

The nominal fuel consumption (in terms of power) $P_\mathrm{f}^\mathrm{nom}$ for an internal combustion engine running at its operating temperature is commonly described by its mechanical efficiency $\eta_\mathrm{e}(\omega_\mathrm{e}, \tau_\mathrm{e})$, as a static function of its rotational

speed $\omega_{\rm e}$ and generated torque $\tau_{\rm e}$, so $P_{\rm f}^{\rm nom} = P_{\rm e}/\eta_{\rm e}$. The temperature-dependency of the fuel consumption, caused by hydrodynamic viscosity effects between moving parts, can be modeled by extending the nominal fuel consumption model using a multiplier function as in [8], so that $P_{\rm f} = \mu_{\rm e}(\vartheta_{\rm p})P_{\rm f}^{\rm nom}$. The multiplier $\mu_{\rm e}$ as a function of the powertrain temperature $\vartheta_{\rm p}$ is modeled by

$$\mu_{\rm e}(\vartheta_{\rm p}) = \begin{cases} 1 + c_{\rm e,1}(\overline{\vartheta}_{\rm p} - \vartheta_{\rm p})e^{c_{\rm e,2}(\overline{\vartheta}_{\rm p} - \vartheta_{\rm p})} & \text{if } \vartheta_{\rm p} < \overline{\vartheta}_{\rm p}, \\ 1 & \text{if } \vartheta_{\rm p} = \overline{\vartheta}_{\rm p} \end{cases}, \tag{3}$$

where $c_{\rm e,1}$ and $c_{\rm e,2}$ are constant coefficients to be identified with the experiments as described next.

C. Temperature-dependent transmission losses

The transmission efficiency of a CVT running at its operating temperature is commonly described by the nominal power dissipation $P_{\rm t}^{\rm nom}$, as a static function of the speed, torque, and speed ratio. For a hydraulically actuated CVT, the power dissipation increases with lower operating temperatures, caused by hydrodynamic viscosity effects in the pump and between moving parts. The temperature-dependency of the power dissipation can be modeled by extending the nominal power dissipation model using a multiplier function as in [8], similar to the fuel consumption model, so that $P_{\rm t} = \mu_{\rm t}(\vartheta_{\rm p})P_{\rm t}^{\rm nom}$. The multiplier $\mu_{\rm t}$ as a function of the powertrain temperature $\vartheta_{\rm p}$ is modeled by

$$\mu_{\rm t}(\vartheta_{\rm p}) = \begin{cases} 1 + c_{\rm t,1}(\overline{\vartheta}_{\rm p} - \vartheta_{\rm p})e^{c_{\rm t,2}(\overline{\vartheta}_{\rm p} - \vartheta_{\rm p})} & \text{if } \vartheta_{\rm p} < \overline{\vartheta}_{\rm p}, \\ 1 & \text{if } \vartheta_{\rm p} = \overline{\vartheta}_{\rm p} \end{cases}, \tag{4}$$

where $c_{\rm t,1}$ and $c_{\rm t,2}$ are constant coefficients to be identified with the experiments as described in the sequel.

D. Coefficient identification

The coefficients $c_{\rm h}$, $\{c_{\rm e,1}, c_{\rm e,2}\}$, and $\{c_{\rm t,1}, c_{\rm t,2}\}$, for, respectively, the models given by (2), (3), and (4), are identified with experiments on two dedicated test rigs. The experiments for the powertrain temperature and the excess fuel consumption are performed on a test rig equipped with a gasoline 2.0-L spark ignition internal combustion engine in series with a mass-produced pushbelt CVT and an Eddy current brake, as described in [22]. The throttle valve position, the CVT speed ratio, and the brake torque are controlled to track the NEDC. The clutch remains engaged during the experiments, mainly for practical reasons, which has a negligible influence on the oil temperature and fuel consumption, since the generated engine power remains the same. Two experiments are performed, starting with a cold powertrain of 20° C and starting with a warm powertrain of 90° C.

The experiments for the excess power dissipation in the transmission are performed on a test rig equipped with a mass-produced pushbelt driven CVT mounted between two electric machines, as described in [23]. The speed and torque of the electric machines as well as the speed ratio of the CVT are controlled to resemble the operating conditions of four constant vehicle velocities of 30 km/h, 50 km/h, 80 km/h, and 120 km/h. The experiments are performed for different temperatures of the transmission oil ranging between 30° C and 80° C.

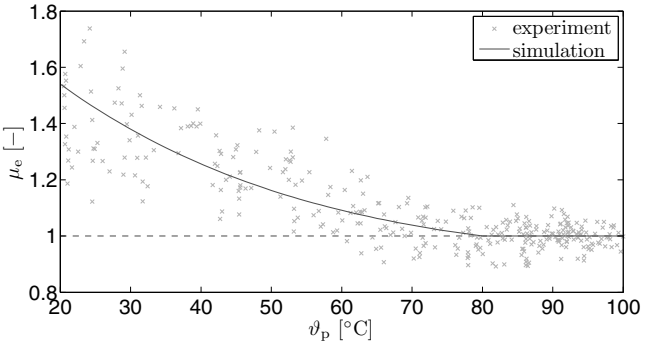

Fig. 2. The excess fuel consumption of the engine ($\mu_{\rm e}$) as a function of the lubrication oil temperature ($\vartheta_{\rm p}$).

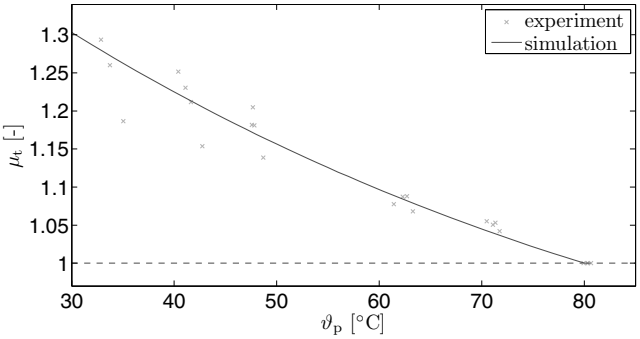

Fig. 3. The excess power dissipation of the transmission ($\mu_{\rm t}$) as a function of the lubrication oil temperature ($\vartheta_{\rm p}$).

Figs. 2 and 3 show, respectively, the measured multiplier functions for the fuel consumption $\mu_{\rm e}$ and the transmission loss $\mu_{\rm t}$, together with their simulated values using (3) and (4). The fuel consumption multiplier ($\mu_{\rm e}$) is corrected for the (implicit) excess power dissipation in the CVT, to isolate the effects of each contribution. The coefficients $c_{\rm e,1}$, $c_{\rm e,2}$, $c_{\rm t,1}$ and $c_{\rm t,2}$ are obtained with least-square fits through the experimental data. It is observed that the excess fuel consumption becomes negligible for oil temperatures above 80° C. The operating temperature of the CVT is mainly determined by the thermostat-controlled temperature of the coolant, which is also close to 80° C. So, the (minimum) operating temperature, for which the temperature has negligible influence on the fuel consumption and transmission losses, is determined at $\overline{\vartheta}_{\rm p} = 80^\circ$ C. Using these identified coefficients, a good resemblance is found between the simulations and experiments.

Fig. 4 shows the measured coolant and oil temperatures

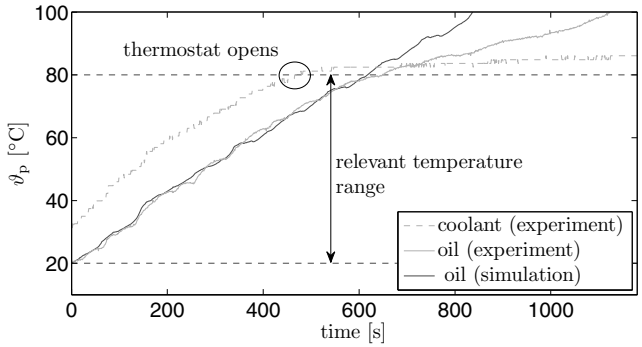

Fig. 4. The coolant and lubrication oil temperature of the engine as a function of time for the NEDC.

TABLE I
THERMODYNAMIC MODEL PARAMETERS

parameter	value	unit	description
$\underline{\vartheta}_p$	20	° C	ambient temperature
$\overline{\vartheta}_p$	80	° C	operating temperature
m_p	180	kg	powertrain mass
A_a	2.60	m^2	powertrain surface
c_a	10	W/m^2K	powertrain heat transfer coefficient
c_p	630	J/kgK	powertrain specific heat coefficient
c_h	0.62	-	powertrain heating coefficient
$c_{e,1}$	3.4	l/kK	fuel consumption coefficient
$c_{e,2}$	16	l/kK	fuel consumption coefficient
$c_{t,1}$	4.2	l/kK	transmission loss coefficient
$c_{t,2}$	7.5	l/kK	transmission loss coefficient
$c_{x,1}$	0.42	-	exhaust gas fraction coefficient
$c_{x,2}$	20	s/krad	exhaust gas fraction coefficient

of the engine for the NEDC, as well as the simulated oil temperature using (2). The operating temperature ($\overline{\vartheta}_p = 80°$ C) is reached shortly after the thermostat opens, so the influence of the radiator is almost negligible during the heating period. As a result, the simulation and experiment resemble quite well for the relevant temperature range, where the powertrain heating coefficient c_h is identified with a least-square fit through the experimental data. The identified coefficients are listed in Table I.

III. HYBRID POWERTRAIN MODEL

The topology of the mechanical hybrid powertrain is schematically depicted in Fig. 5. The main components are a 1.5-l gasoline internal combustion engine, a compact 150-kJ flywheel system, three clutches, a pushbelt CVT, and a compact passenger vehicle including 2 passengers with a total mass of 1120 kg. The modeling of the hybrid powertrain is extensively described in [24] and shortly summarized in the sequel. The longitudinal (motion) dynamics are described for the most relevant inertias, *i.e.*, that of the flywheel and the vehicle. The transmission clutch (C_t) is used to accelerate the vehicle (or, flywheel) from standstill, by transmitting high torques while slipping. The engine clutch (C_e) and flywheel clutch (C_f) are used to (dis-)engagement of powertrain parts, in order to select one of the relevant driving modes ϕ:

- *Flywheel driving*: the flywheel system propels or brakes the vehicle while the engine is shut-off ($\phi = 1$).

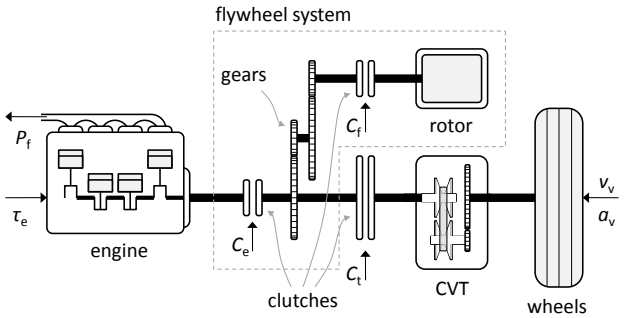

Fig. 5. The mechanical hybrid powertrain topology, which consists of an internal combustion engine, flywheel system, continuously variable transmission, and three clutches.

- *Hybrid driving*: the engine propels the vehicle while energizing the flywheel system ($\phi = 2$).
- *Engine driving*: the engine propels the vehicle while the flywheel system is idling, or the flywheel system brakes the vehicle while the engine is idling ($\phi = 3$).

Physical constraints apply to the torques, the rotational speeds, and the speed ratio of the CVT, whereas comfort-related constraints apply to driving modes and driving mode switches that are expected to be uncomfortable, which depend on the driving conditions.

IV. OPTIMIZATION

The thermodynamics and the energy dynamics of the hybrid powertrain are combined in one dynamic model function f, using a simple forward Euler scheme with a fixed time step of $\Delta t = 1$ s and time index k, *i.e.*,

$$x(k+1) = x(k) + f(x(k), u(k), w(k))\Delta t, \qquad (5)$$

where the state vector $x(k)$ contains the kinetic energy in the rotor of the flywheel system $E_r(k)$, the previous driving mode $\phi_{pre}(k) = \phi(k-1)$, and the powertrain temperature $\vartheta_p(k)$. The control variables $u(k)$ are the current driving mode $\phi(k)$ and the relative power split $\sigma(k)$ in the hybrid driving mode, where $\sigma(k) = 0$ implies no flywheel energizing and $\sigma(k) = 1$ implies maximal flywheel energizing. The external variable vector $w(k)$ contains the vehicle speed $v_v(k)$ and the acceleration, which are prescribed by the driving cycle. The optimal control objective is to minimize the overall fuel consumption, over a prescribed driving cycle of length k_n, given by

$$\min_{u(k)} \sum_{k=0}^{k_n} P_f(x(k), u(k), w(k))\Delta t, \qquad (6)$$

subject to the kinematics, dynamics, the physical operating limits, and comfort-related constraints described in [24]. There is no final state constraint for energy sustenance, as the flywheel system can only store energy for a relatively short term. Dynamic programming is used to find the global optimal solution [16], which is a numerical method that is

TABLE II

SIMULATION SETTINGS

#	setting	initial states $x(0)$	driving mode space
1	conventional, cold	$[3, 0, \underline{\vartheta}_\mathrm{p}]^\mathrm{T}$	$\phi = 3$
2	conventional, warm	$[3, 0, \overline{\vartheta}_\mathrm{p}]^\mathrm{T}$	$\phi = 3$
3	hybrid, cold	$[1, 0, \underline{\vartheta}_\mathrm{p}]^\mathrm{T}$	$\phi \in \{1, 2, 3\}$
4	hybrid, warm	$[1, \overline{E}_\mathrm{r}/2, \overline{\vartheta}_\mathrm{p}]^\mathrm{T}$	$\phi \in \{1, 2, 3\}$

very suitable to deal with the switched non-linear powertrain dynamics and the relatively many constraints.

V. SIMULATIONS

The fuel saving potential of the hybrid powertrain is computed with respect to its conventional (non-hybrid) counterpart. To isolate the fuel saving effects of only the flywheel system from that of other powertrain components, the same powertrain model is used, except for the flywheel system mass of 27 kg, and the possibility of flywheel driving and hybrid driving. These powertrains are evaluated using the following simulation settings:

1) *Conventional powertrain*: the driving mode is restricted to engine driving $\phi = 3$, whereas the power split is redundant.
2) *Hybrid powertrain*: the driving mode and the relative power split are not restricted, so $\phi \in [1, 3]$ and $\sigma \in [0, 1]$.

Two different start conditions are investigated. The *cold start* conditions represent the situation when the vehicle has been parked for a few hours, so the powertrain is at its ambient temperature and the flywheel is stationary. The *warm start* conditions represent the situation when the vehicle has been parked for only a few minutes, so the powertrain is still at operating temperature, whereas the flywheel is still spinning. The two situations are evaluated using the following combinations for the initial states:

1) *Cold start*: the flywheel is stationary ($E_\mathrm{r}(0) = 0$), the powertrain starts in the engine driving mode ($\phi(0) = 3$), and the powertrain temperature equals its ambient temperature ($\vartheta_\mathrm{p}(0) = \underline{\vartheta}_\mathrm{p}$);
2) *Warm start*: the flywheel contains 50% of its capacity ($E_\mathrm{r}(0) = \overline{E}_\mathrm{r}/2$), the powertrain starts in the flywheel driving mode ($\phi(0) = 1$), and the powertrain is at its operating temperature ($\vartheta_\mathrm{p}(0) = \overline{\vartheta}_\mathrm{p}$).

The four simulation settings are summarized in Table II. Each simulation is performed for six representative driving cycles, which are the New European Driving Cycle (NEDC), the Federal Test Procedure '75 (FTP75), the Japan Cycle 08 (JC08), the "low", "medium", and "high" parts of the Worldwide harmonized Light vehicles Test Procedure (WLTP), the "urban" part of the Common Artemis Driving Cycle (CADC), and the sportive Eindhoven driving cycle (EHV).

VI. RESULTS & DISCUSSION

A. Fuel consumption

Fig. 6 shows the impact of the cold start conditions on the fuel consumption of both the hybrid and conventional powertrain in the top graph, and on the fuel saving potential of the hybrid powertrain with respect to the conventional powertrain in the bottom graph. The cold start has a significant impact on the fuel consumption for the conventional powertrain ($5.0\% - 12.0\%$) and even a higher impact for the hybrid powertrain ($8.9\% - 29.4\%$) due to the intermittent and solely efficient engine operation. As expected, the highest fuel saving potential is observed with the warm start ($20.2\% - 40.6\%$), especially for the three urban driving cycles (EHV, JC08, and CADC) that contain many fuel saving possibilities ($32.6\% - 40.6\%$). The three other driving cycles show a lower fuel saving potential, due to the highway parts for which the conventional powertrain is already efficient ($20.2\% - 24.8\%$). Despite the significant impact of the cold start conditions ($3.5\% - 9.2\%$), the optimally controlled mechanical hybrid powertrain still has a relatively high fuel saving potential of between $14.7\% - 31.4\%$, which depends on the driving cycle.

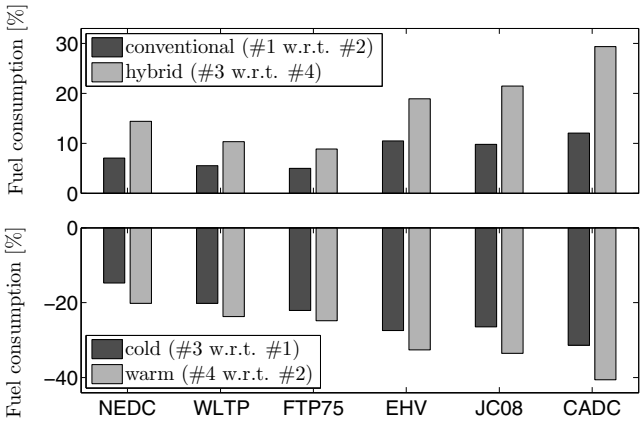

Fig. 6. The impact of the cold start conditions on the fuel consumption (top) and on the fuel saving potential of the hybrid powertrain (bottom), evaluated for six driving cycles.

B. Energy management strategy

Fig. 7 shows, respectively, from top to bottom, the vehicle velocity (v_v), driving mode (ϕ), the relative power split (σ), the kinetic flywheel energy (E_f), and the powertrain temperature (ϑ). As expected, the hybrid powertrain has a significantly longer heating time (30%) compared to the conventional powertrain due to intermittent and efficient engine operation (see, ϑ_p). The initially stationary flywheel restricts the hybrid powertrain with the cold start conditions to engine driving for the first 160 s (see, ϕ), until sufficient brake energy is recuperated to enable the other driving modes. After this initialization, the flywheel energy (see, E_r) converges to the same trajectory as for the warm start conditions. This behavior is observed for all driving cycles and shows that the cold powertrain temperature has a negligible influence on the optimal EMS.

The overall fuel consumption can be improved by faster heating of the powertrain, in order to reduce the excess fuel consumption and excess transmission loss. Faster heating, however, can only be realized by temporary decreasing the

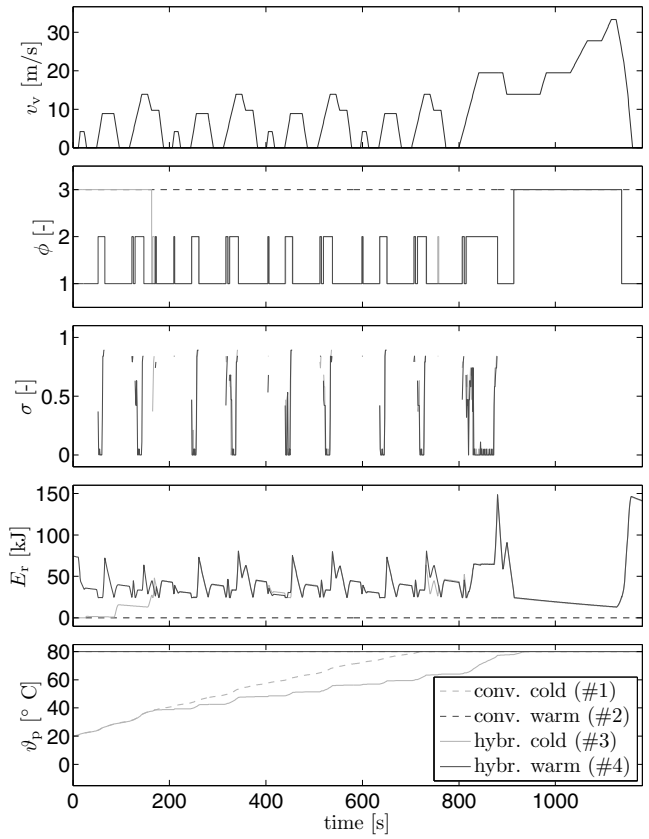

Fig. 7. Results for the NEDC. (Top to bottom) The velocity of the vehicle (v_v), the driving mode (ϕ), the relative power split (σ), the kinetic flywheel energy (E_r), and the powertrain temperature (ϑ).

mechanical efficiency, which is not effective to reduce the overall fuel consumption, or by temporary increasing the engine power by using the energy buffer, so that the CVT efficiency increases before the stored energy is transmitted through the CVT. The latter effect may be advantageous when using a large energy buffer, yet not for the relatively small energy storage capacity (150 kJ) of the mechanical-hybrid powertrain. As a result, the energy buffer is used similarly as with the warm start (see, E_r), where the excess power loss of the CVT is compensated by slightly prolonging the hybrid mode (see, ϕ) and altering the relative power split in this mode (see, σ). Based on these insights, the temperature state can be eliminated from the state space, which substantially simplifies the design of a real-time implementable EMS. The impact on other temperature-dependent criteria such as exhaust gas emissions and acceleration performance are interesting topics recommended for further investigation.

REFERENCES

[1] A. Sciarretta and L. Guzzella, "Control of hybrid electric vehicles," *IEEE Control Systems*, vol. 27, no. 2, pp. 60–70, 2007.

[2] D. Bolis, J. Johnson, and R. Callen, "A study on the effect of oil and coolant temperatures on diesel engine brake specific fuel consumption," *SAE Technical Paper 770313*, 1977.

[3] G. E. Andrews, J. R. Harris, and A. Ounzain, "Si engine warm-up: Water and lubricating oil temperature influences," *SAE Technical Paper 892103*, 1989.

[4] P. Shayler, S. Christian, and T. Ma, "A model for the investigation of temperature, heat flow and friction characteristics during engine warm-up," *SAE Technical Paper 931153*, pp. 667–675, 1993.

[5] T. Morel and R. Keribar, "Warmup characteristics of a spark ignition engine as a function of speed and load," *SAE Technical Paper 900683*, 1990.

[6] K. Kunze, S. Wolff, I. Lade, and J. Tonhauser, "A systematic analysis of co2-reduction by an optimized heat supply during vehicle warm-up," *SAE Technical Paper 2006-01-1450*, vol. 01, 2006.

[7] G. Vogelaar, "Vt2+: further improving the fuel economy of the vt2 transmission," in *Proc. of the 6th Int. Conf. on Continuously Variable and Hybrid Transmissions, Maastricht, Netherlands*, 2010, pp. 105–109.

[8] D. Kok, "Design optimization of a flywheel hybrid vehicle," Ph.D. dissertation, Technische Universiteit Eindhoven, Netherlands, 1999.

[9] C. Haupt, D. Bücherl, A. Engstle, H.-G. Herzog, and G. Wachtmeister, "Energy management in hybrid vehicles considering thermal interactions," in *Proc. of the Vehicle Power and Propulsion Conference, Arlington, Texas, U.S.A.*, 2007, pp. 36–41.

[10] T. Mueller, H. Hans, W. Krebs, S. Smith, and A. Koenigstein, "Thermal management on small gasoline engines," *SAE International*, no. 2011-01-0314, 2011.

[11] F. Will and A. Boretti, "A new method to warm up lubricating oil to improve the fuel efficiency during cold start," *SAE International*, no. 2011-01-0318, 2011.

[12] R. Cipollone, D. D. Battista, and A. Gualtieri, "Head and block split cooling in internal combustion engines," in *in Proc. of the IFAC Workshop on Engine and Powertrain Control, Simulation and Modeling*, 2012, pp. 469–476.

[13] E. Muller, A. Stefanopoulou, and L. Guzzella, "Optimal power control of hybrid fuel cell systems for an accelerated system warm-up," *IEEE Transactions on Control Systems Technology*, vol. 15, no. 2, pp. 290–305, 2007.

[14] J. Lescot, A. Sciarretta, Y. Chamaillard, and A. Charlet, "On the integration of optimal energy management and thermal management of hybrid electric vehicles," in *Proc. of the Vehicle Power and Propulsion Conference, Lille, France*, 2010, pp. 1–6.

[15] R. Dubouil, J. F. Hetet, and A. Maiboom, "Modelling of the warm-up of a spark ignition engine: Application to hybrid vehicles," *SAE International*, no. 2011-01-1747, 2011.

[16] D. P. Bertsekas, *Dynamic Programming and Optimal Control, Volume 1*, 3rd ed. Athena Scientific, Belmont, Massachusetts, U.S.A., 2005.

[17] J. A. Kaplan and J. B. Heywood, "Modeling the spark ignition engine warm-up process to predict component temperatures and hydrocarbon emissions," in *SAE International Congress and Exposition, Detroit, Michigan, U.S.A.*, no. 910302, 1991.

[18] O. Arici, J. H. Johnson, and A. J. Kulkarni, "The vehicle engine cooling system simulation part 1 - model development," in *SAE World Congress and Exposition, Detroit, Michigan, U.S.A.*, no. 1999-01-0240, 1999.

[19] L. Jarrier, J. C. Champoussin, R. Yu, and D. Gentile, "Warm-up of a d.i. diesel engine: Experiment and modeling," in *SAE World Congress, Detroit, Michigan*, 2000.

[20] L. Guzzella and C. Onder, *Introduction to Modeling and Control of Internal Combustion Engine Systems*, 2nd ed. Springer-Verlag, 2010.

[21] T. Markel, A. Brooker, T. Hendricks, V. Johnson, K. Kelly, B. Kramer, M. O'Keefe, S. Sprik, and K. Wipke, "Advisor: a systems analysis tool for advanced vehicle modeling," *Journal of Power Sources*, vol. 110, no. 2, pp. 255–266, 2002.

[22] R. Eichhorn, M. Boot, and C. Luijten, "Waste energy driven air conditioning system (wedacs)," *SAE Int. J. of Engines*, vol. 2, no. 2, pp. 477–492, 2009, 2009-24-0063.

[23] K. van Berkel, T. Hofman, B. Vroemen, and M. Steinbuch, "Optimal regenerative braking with a push-belt CVT: an experimental study," in *Proc. of the 10th Int. Symp. on Advanced Vehicle Control, Loughborough, U.K.*, 2010, pp. 67–72.

[24] ——, "Optimal control of a mechanical-hybrid powertrain," *IEEE Transactions On Vehicular Technology*, vol. 61, no. 2, pp. 485–497, 2012.